Spring 5-15-2015

Three-Dimensional Ideal Gas Reference State based Energy Function

Avdesh Mishra
University of New Orleans, amishra2@uno.edu

Three-Dimensional Ideal Gas Reference State based Energy Function

A Thesis

Submitted to the Graduate Faculty of the
University of New Orleans
In partial fulfillment of the
Requirements for the degree of

Master of Science
in
Computer Science

by

Avdesh Mishra

BS in Computer Engineering, Tribhuvan University, 2012

May, 2015

Table of Contents

List of Figures iii
List of Tables iv
ABSTRACT v
INTRODUCTION 1
MATERIALS and METHODS 3
Residue Specific All-Atom Probability Discriminatory Function based Potential 3
DFIRE Based Potential 6
3DIGARS, the Proposed Approach 8
GA over Grid Search for Optimal Parameter 13
DATASET COLLECTION and DECOY DATASETS 14
Training Dataset 14
Decoy Datasets 16
Moulder Decoy-set 17
Rosetta Decoy-set 17
I-Tasser Decoy-set-II 17
4state_reduced 18
Fisa 18
Fisa_casp3 18
Hg_structal 18
Ig_structal 18
Ig_structal_hires 19
Lattice_ssfit 19
Lmds 19
RESULTS 19
CONCLUSIONS 22
SUPPLEMENTARY CONTENT 23
REFERENCES 23
VITA 26

List of Figures

FIGURE 1: (A) NATIVE LIKE PROTEIN CONFORMATION [25], PRESENTED IN A 3D HEXAGONAL-CLOSE-PACKING (HCP) CONFIGURATION USING HYDROPHOBIC (H) AND HYDROPHILIC OR POLAR (P) RESIDUES. THE H-H INTERACTIONS SPACE IS RELATIVELY SMALLER THAN P-P INTERACTIONS SPACE, SINCE HYDROPHOBIC RESIDUES (BLACK BALL) BEING AFRAID OF WATER TENDS TO REMAIN INSIDE OF THE CENTRAL SPACE. (B) 3D METAPHORIC HP FOLDING KERNELS, DEPICTED BASED ON HCP CONFIGURATION BASED HP MODEL, SHOWING THE 3 LAYERS OF DISTRIBUTIONS OF AMINO-ACIDS [25], [26]. 3

FIGURE 2: FITNESS VERSUS A_HP, A_HH AND A_PP VALUES. THE VALUES REMAIN STABLE DURING OPTIMIZATION, ENSURE RELIABILITIES. 13

List of Tables

TABLE 1: HYDROPHOBIC (H)/ HYDROPHILIC (P) CATEGORIZATION OF THE AMINO ACIDS. 10
TABLE 2: PERFORMANCE OF TWO DIFFERENT REFERENCE STATE ON TRAINING DATASET DIFFERED BY MAXIMUM RESOLUTION AND SIMILARITY CUTOFF WHILE KEEPING OTHER PARAMETERS SUCH AS EXPERIMENTAL METHOD AS "IGNORE", MOLECULE TYPE AS "PROTEIN", REFINEMENT R-FREE OF MINIMUM 0.0 AND MAXIMUM 0.25 , NUMBER OF CHAINS AS "SINGLE CHAIN" IF NOT MENTIONED. 20
TABLE 3: COMPARISON BETWEEN DFIRE, RWPLUS, DDFIRE, DFIRE2.0 AND OUR ENERGY FUNCTION (3DIGARS) ON 11 DECOY SETS BASED ON CORRECT SELECTION OF NATIVE FROM THEIR DECOY SET AND Z-SCORE. 21
TABLE 4: COMPARISON BETWEEN DFIRE, RWPLUS, DDFIRE, DFIRE2.0 AND OUR ENERGY FUNCTION (3DIGARS) BASED ON CORRECT SELECTION OF NATIVE FROM THEIR DECOY SET AND Z-SCORE. 22

ABSTRACT

Energy functions are found to be a key of protein structure prediction. In this work, we propose a novel 3-dimensional energy function based on hydrophobic-hydrophilic properties of amino acid where we consider at least three different possible interaction of amino acid in a 3-dimensional sphere categorized as hydrophilic versus hydrophilic, hydrophobic versus hydrophobic and hydrophobic versus hydrophilic. Each of these interactions are governed by a 3-dimensional parameter alpha used to model the interaction and 3-dimensional parameter beta used to model weight of contribution. We use Genetic Algorithm (GA) to optimize the value of alpha, beta and Z-score. We obtain three energy scores libraries from a database of 4332 protein structures obtained from Protein Data Bank (PDB) server. Proposed energy function is found to outperform nearest competitor by 40.9% for the most challenging Rosetta decoy as well as better in terms of the Z-score based on Moulder and Rosetta decoy sets.

KEYWORDS: protein structure, energy function, optimization, genetic algorithm, decoy-set.

INTRODUCTION

History of protein structure prediction is based on the thermodynamic hypothesis that the native structure gains the lowest free energy compared to the other decoys or the intermediate conformations under same physiological conditions [1]. A decent potential that can discriminate between native and nearly infinite number of possible decoy structures is vital for protein structure prediction. So far many attempts have been made towards development of better energy function which can be categorized into two different types [2; 3; 4; 5; 6] *i*) physical-based potential, based on molecular dynamics or computation of atom-atom forces [7; 8]; and *ii*) knowledge-based potentials, obtained from statistical analysis of known protein structure [9; 10; 11; 12; 13; 14]. Some of the energy functions are modelled based on only backbone alpha carbon atom whereas, many of these are based on all atom (167 heavy atoms), knowledge based, distance dependent potential. They vary from one another based on the reference state and the type of physical features they employ to counterbalance sampling bias [15]. For example, Kortemme et al. [16] obtained a knowledge-based hydrogen-bonding potential. Yang and Zhou incorporated polar-polar and polar-nonpolar orientation dependence to the distance-dependent knowledge-based potential based on a distance-scaled, finite-ideal gas reference (DFIRE) state [17] by treating polar atoms as a dipole (dDFIRE) [18]. Lu et al. [19] defined side-chain orientation according to rigid blocks of atoms (OPUS-PSP). Zhang and Zhang [20] employed orientation angles between two vector pairs predefined for each side-chain (RWplus). Zhou and Skolnick improved over the DFIRE energy function by incorporating relative orientation of the planes associated with each heavy atom (GOAP) [21]. For obvious reasons, the relatively complete and detail approaches are the all atom based approaches. The efficacy of the all-atom based approach relay heavily on the formulation of the more accurate reference state [15]. Our proposed work in this paper, focuses on all-atom as

well as knowledge based approach that derives an effective energy function from known protein structures with multidimensional reference states.

We propose an improved potential based on four factors *i)* better training dataset; *ii)* three different energy scores based on hydrophobic and hydrophilic categorization of residue-atom pairs; *iii)* three different alpha values for three different energy scores generation; and *iv)* three different weights of contribution of energy scores. Fundamental work of DFIRE considers residues placed in a modified spherical environment controlled by the single dimensional parameter (alpha), where the alpha value is used to calculate the volume of the sphere considering the spherical environment as a finite system [10]. On the contrary, our motivation towards this work comes from the fact that – amino acids, based on their types are not distributed equally over the 3D structure of a protein to consider them in the same scale on an average by a single dimensional parameter (see Fig. 1(a)). Rather they can be segregated into at least 3 different categories based on the usual distribution with the protein conformations (see Fig. 1(b)). Related to this, hydrophobic-hydrophilic or hydrophobic-polar (HP) model considers hydrophobic (H) amino acids having fear of solvent like water, they want to keep themselves away from aqueous solvent forming the core or inner-kernel [22] of protein and thus remain inside of a protein. On the other hand, the hydrophilic or the polar (P) amino acid or residues being attracted to water, try to remain outside the core, forming the outer-kernel (see Fig. 1 (b)). Thus Ps are often found on the outside of their folded structure [23; 24], and in between this two layer there is a thin HP-mixed-layer [22]. Following these aforementioned properties, we proposed our multidimensional reference states based energy function 3DIGARS (3 Dimensional Ideal Gas Reference State) for improved accuracy.

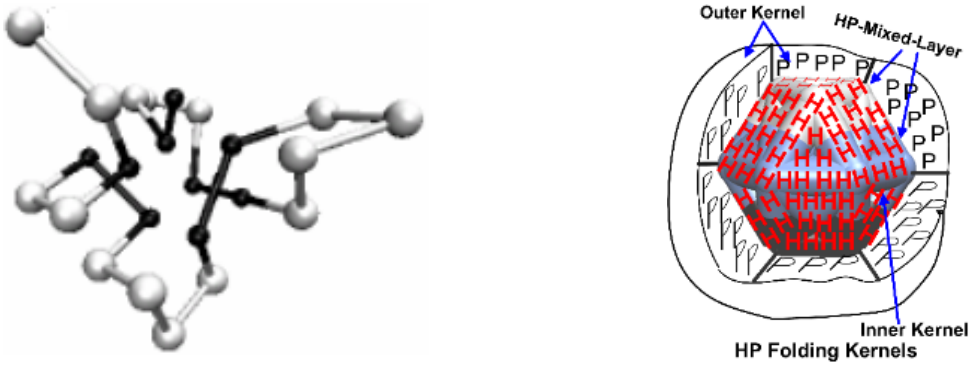

(a) (b)

Figure 1: (a) Native like protein conformation [25], presented in a 3D hexagonal-close-packing (HCP) configuration using hydrophobic (H) and hydrophilic or polar (P) residues. The H-H interactions space is relatively smaller than P-P interactions space, since hydrophobic residues (black ball) being afraid of water tends to remain inside of the central space. (b) 3D metaphoric HP folding kernels, depicted based on HCP configuration based HP model, showing the 3 layers of distributions of amino-acids [25], [26].

The remainder of this paper proceeds as follows. We review the evolution of the relevant theories and underpinning theoretical aspect of our proposed approaches in Section 2. Section 3 discusses our approach for training data collections as well as the collections of the decoy-datasets to be used for measuring performances of our approach compared to other state-of-art-approaches. We discussed the obtained results in Section 4 and finally Section 5 concludes the proposed energy function.

MATERIALS and METHODS

Residue Specific All-Atom Probability Discriminatory Function based Potential

Initially, the residue specific all-atom probability discriminatory function (RAPDF) based energy function was proposed by Samudrala and Moult [9] which was based on averaging reference state. In this approach, the energy score of a conformation was computed in two different ways: conditional probability based approach and free energy based approach. It was found that these two approaches are equivalent for all practical purposes while it is more easier to work with conditional probability based approach because, of the Boltzmann assumption on three different

aspect of it: an equilibrium distribution of atom pairs, the physical nature of the reference state and the probability of observing a system in any given state which is also subject to change with respect to the temperature [2].

Conditional probabilities of pairwise atom-atom interactions in proteins can be computed using statistical observation of native structures [9] from protein-databases such as Protein Data Bank [27]. The conditional probabilities are based on two different type of structures one which is native (N) and the other is the near native or decoy (D). Energy potentials are developed based on the pairwise atom-atom interactions of native structures. Pairwise atom-atom distance is a set of intra-atomic separation within a structure represented as $\{S_{ab}^{ij}\}$, where $\{S_{ab}^{ij}\}$ is the distance between atom *i* and *j* of amino acid type *a* and *b*, respectively. The probability that the atom pairs separated by distance $\{S_{ab}^{ij}\}$ belongs to native conformation can be represented by $P(N \mid S_{ab}^{ij})$. Therefore, we can write the general formula of conditional probability that, atom pairs separated by distance $\{S_{ab}^{ij}\}$ belongs to native conformation as:

$$P(N \mid S_{ab}^{ij}) = (P(S_{ab}^{ij} \mid N) * P(N)) / P(S_{ab}^{ij}) \tag{1}$$

Assuming that all distances are independent of each other, conditional probabilities can be expressed as the probabilities of observing the set of distances as products of the probabilities of observing each individual distance [9]

$$P(S_{ab}^{ij} \mid N) = \prod_{ij} P(S_{ab}^{ij} \mid N) \text{ and } P(S_{ab}^{ij}) = \prod_{ij} P(S_{ab}^{ij}) \tag{2}$$

Substituting the Eq. 1 by Eq. 2 we get Eq. 3:

$$P(N \mid S_{ab}^{ij}) = P(N) * \prod_{ij} P(S_{ab}^{ij} \mid N) / P(S_{ab}^{ij}) \tag{3}$$

$P(N)$ in above equation is a constant and independent of conformation of given structure and so it can be omitted from further consideration. Omission of $P(N)$ implicates that scores from different sequences cannot be compared. Thus the log form of Eq. 3 is used to both scale the quantities to a small range and to give a form similar to that of potential of mean force. Scoring function *SF* proportional to the negative log conditional probability that the structure is correct can be written as:

$$SF(\{S_{ab}^{ij}\}) = -\sum_{ij} \ln P(S_{ab}^{ij} \mid N) / P(S_{ab}^{ij}) K - \ln P\left(N \mid \{S_{ab}^{ij}\}\right) \tag{4}$$

Therefore, given a protein structure or conformation, using Eq. 4, we can calculate all the distance separation between all pairs of atom types and compute the total energy by summing up the probability ratios assigned to each separation between a pair of atom types. Thus, we can compute the probability of observing atom type *a* and *b* in a particular bin which is *S* distance apart in a native conformation $P(S_{ab} \mid N)$ as:

$$P(S_{ab} \mid N) = N(S_{ab}) / \sum_{s} N(S_{ab}) \tag{5}$$

where $N(S_{ab})$ is the frequency of observation of atom type *a* and *b* in a particular bin which is of *S* distance apart. The denominator is the number of such observation for all bins.

The denominator in Eq. 5 is the average over different atom types in the experimental conformations which represents the random reference state. Thus the probability of seeing any two atom types *a* and *b* in a bin which is *S* distance apart can be represented as:

$$P(S_{ab}) = \sum_{ab} N(S_{ab}) / \sum_{S} \sum_{ab} N(S_{ab}) \tag{6}$$

where, $\sum_{ab} N(S_{ab})$ is the total number of counts summed over all pairs of atom types in a particular distance *S*, and the denominator is the total number of counts summed over all pairs of atom types summed over all bins.

As RAPDF energy function is based on averaging reference state, it does not consider the distribution of amino acid in 3D conformational space whereas DFIRE based potential considers protein as a sphere comprising of uniformly distributed atoms and also suggest that the radius of such spheres does not increase in r^2 as in an infinite system rather protein is a finite system and so the increase in the radius is represented by α (a variable which can be ≤ 2). This involved our concerns toward more detailed study into DFIRE based potential.

DFIRE Based Potential

Distance-scaled, finite ideal-gas reference (DFIRE) state is a distance-dependent, all atom, knowledge-based potential [10]. The reference state formulation in DFIRE is more appealing and effective over RAPDF. The reference state RAPDF uses an averaged distribution over all residue or atom pairs whereas, DFIRE uses pair distribution function from statistical mechanics to formulate finite ideal-gas reference state.

The basis of finite ideal-gas reference state can be explained by exploring the fundamental equation of statistical mechanics for infinite system. For an infinite system the observed number of pairs of atoms, namely i^{th} and j^{th} atoms, denoted as $N_{obs}(i,j,d)$, at spatial distance *d* with tolerance ±Δ*d* is related to the pair distribution function $g_{ij}(d)$, which describes how density varies as a function of distance from a reference particle and can be represented as:

$$N_{obs}(i,j,d) = \frac{1}{v^s} N_i^s N_j^s g_{ij}(d)(4\pi d^2 \Delta d) \tag{7}$$

where volume of the system is represented as v^s, N_i^s and N_j^s are the number of i^{th} and j^{th} atoms in a system, respectively. The potential based on pairwise distance $P(i,j,d)$ can be written as:

$$P(i,j,d) = -RT\ln((N_{obs}(i,j,d)*V^s)/(N_i^s N_j^s(4\pi d^2\Delta d))) \quad (8)$$

In case there is no interaction between the atoms, we can write: $P(i,j,d) = 0$, thus from Eq. 8 we can have:

$$N_{\exp}(i,j,d) = N_{obs}(i,j,d) = N_i^s N_j^s(4\pi d^2\Delta d / v^s) \quad (9)$$

Equations above from statistical mechanics can directly be applied in infinite system whereas the proteins are finite system, therefore, the pair density will not increase by square factor (i.e., d^2), rather it increase by some factor α (i.e., d^α) which was determined by the best fit of d^α considering number of points in 1011 finite protein size spheres.

Thus, Eq. 9 can be written as:

$$N_{\exp}(i,j,d) = N_i^s N_j^s(4\pi d^\alpha\Delta d / v^s) \quad (10)$$

Further, Eq. 8 can be rewritten as:

$$P(i,j,d) = -RT\ln((N_{obs}(i,j,d)*V^s)/(N_i^s N_j^s(4\pi d^\alpha\Delta d))) \quad (11)$$

Assuming that there is no interaction beyond cutoff distance of d_{cut} or $P(i,j,d) = 0$ at $d \geq d_{cut}$, d is replaced by d_{cut}. This leads Eq. 11 to form Eq. 12:

$$P(i,j,d) = -\eta RT\ln\frac{N_{obs}(i,j,d)}{\left(\frac{d}{d_{cut}}\right)^\alpha \frac{\Delta d}{\Delta d_{cut}} N_{obs}(i,j,d_{cut})} \quad (12)$$

Here, a constant η is placed for mutation induced changes and is also needed because temperature is a free parameter in potentials derived from static structures. Eq. 12 implies new equation for $N_{\exp}(i,j,d)$:

$$N_{\exp}(i,j,d) = \left(\frac{d}{d_{cut}}\right)^{\alpha} \frac{\Delta d}{\Delta d_{cut}} N_{obs}(i,j,d_{cut}) \tag{13}$$

It is to be noted that the Eq. 13 does not contains any distance dependent term rather it is a formulation obtained from ideal gas reference state implementable for finite system.

Similar to the approaches in Samudrala and Moult [9], DFIRE also uses 167 heavy atom types. The cutoff distance d_{cut} is = 14.5 Å. The bin width Δd have different width for d < 2 Å, Δd=2 Å, for 2 Å < d < 8 Å, Δd=0.5 Å and for 8 Å < d < 15 Å, Δd=1 Å. Thus, the total number of bins is 20. Bin width and d_{cut} were not optimized.

3DIGARS, the Proposed Approach

Based on the hydrophobic-hydrophilic model (HP model) we constructed three different energy score libraries with bin size, Δr = 0.5 Å each, with a cutoff distance of 15 Å, where r represents each distant bin with values ranging from 0.5 Å to 15 Å. The value of cutoff bin Δr_{cut} = 0.5 Å as all bin size are same. Residue-atom pairs within same residue were ignored while constructing energy score libraries. We name these libraries as *i*) hydrophobic-hydrophilic (HP); *ii*) hydrophobic-hydrophobic (HH); and *iii*) hydrophilic-hydrophilic (PP) interactions libraries and each of these libraries comprises of its independent reference state. Reference state corresponding to hydrophobic-hydrophilic group can be written as:

$$N_{i,j}^{EXP-HP}(r) = \left(\frac{r}{r_{cut}}\right)^{\alpha_{hp}} \frac{\Delta r}{\Delta r_{cut}} (N_{obs-HP}(i,j,r_{cut}) + N_{obs-HH}(i,j,r_{cut}) + N_{obs-PP}(i,j,r_{cut})) \tag{14}$$

where $N_{i,j}^{EXP-HP}(r)$ represents the expected number of atom pairs at distance *r* for hydrophobic versus hydrophilic interaction, $N_{obs-HP}(i,j,r_{cut})$ represents observed number of atom pairs i^{th} and j^{th} at cutoff distance in hydrophobic-hydrophilic library, $N_{obs-HH}(i,j,r_{cut})$ represents observed number of atom pairs i^{th} and j^{th} at cutoff distance in hydrophobic-hydrophobic library, $N_{obs-PP}(i,j,r_{cut})$ represents observed number of atom pairs i^{th} and j^{th} at cutoff distance from hydrophilic-hydrophilic library and α_{hp} is the parameter that belongs to hydrophobic versus hydrophilic group which is obtained by GA.

Similarly, reference state corresponding to hydrophobic-hydrophobic group can be written as:

$$N_{i,j}^{EXP-HH}(r) = \left(\frac{r}{r_{cut}}\right)^{\alpha_{hh}} \frac{\Delta r}{\Delta r_{cut}} (N_{obs-HP}(i,j,r_{cut}) + N_{obs-HH}(i,j,r_{cut}) + N_{obs-PP}(i,j,r_{cut})) \quad (15)$$

where $N_{i,j}^{EXP-HH}(r)$ represents the expected number of atom pairs at distance *r* for hydrophobic versus hydrophobic interaction, α_{hh} is the parameter that belongs to hydrophobic versus hydrophobic group which is also obtained by GA and rest of the terms are as defined under Eq. 14.

Finally, reference state corresponding to hydrophilic-hydrophilic group can be written as:

$$N_{i,j}^{EXP-PP}(r) = \left(\frac{r}{r_{cut}}\right)^{\alpha_{pp}} \frac{\Delta r}{\Delta r_{cut}} (N_{obs-HP}(i,j,r_{cut}) + N_{obs-HH}(i,j,r_{cut}) + N_{obs-PP}(i,j,r_{cut})) \quad (16)$$

where $N_{i,j}^{EXP-PP}(r)$ represents the expected number of atom pairs at distance *r* for hydrophilic versus hydrophilic group, α_{pp} is the parameter that belongs to hydrophilic-hydrophilic group which is also obtained by GA and rest of the terms are as defined under Eq. 14.

While generating energy score libraries, residue-atom pairs are categorized to identify which of the group (HP, HH or PP) mentioned above they fall in e.g. while considering interaction between two Nitrogen (N) atom of amino acid Alanine (ALA:N versus ALA:N), we categorize this interaction as hydrophobic-hydrophobic (HH) group as amino acid ALA (Alanine) is hydrophobic in nature. Similarly, while considering interaction between Nitrogen (N) atom of amino acid Arginine (ARG) and Carbon (C) atom of amino acid Serine (SER); (ARG:N versus SER:C), we categorize this interaction as hydrophilic-hydrophilic (PP) as both residues Arginine (ARG) and Serine (SER) are hydrophilic in nature. The categorization of amino acid into hydrophobic and hydrophilic group is obtained from [24] also shown in Table 1.

Table 1: Hydrophobic (H)/ Hydrophilic (P) categorization of the amino acids.

S. No.	Amino Acid (3-letter Code)	Group as Hydrophobic (H) /Hydrophilic (P)
1	ARG	P
2	ASN	P
3	ASP	P
4	CYS	P
5	GLN	P
6	GLU	P
7	LYS	P
8	HIS	P
9	PRO	P
10	SER	P
11	THR	P
12	TRP	P
13	TYR	H
14	VAL	H
15	GLY	H
16	ALA	H
17	ILE	H
18	LEU	H
19	MET	H
20	PHE	H

Along with the categorization of residue-atom pairs the frequency counts of the specific group is updated simultaneously. Further these energy score libraries are used for total energy or minimum energy calculation. Once we compute frequencies of all the 3 groups, we generate energy scores corresponding to each group. Energy score for HP group can be written as:

$$ES_{i,j,r}^{HP} = -\ln(N_{obs-HP}(i,j,r) / N_{i,j}^{EXP-HP}(r)) \quad (17)$$

where $ES_{i,j,r}^{HP}$ is the energy score of atom pair i^{th} and j^{th} at distant bin r for group HP, $N_{obs-HP}(i,j,r)$ is the observed number of atom pair i^{th} and j^{th} at distant bin r for HP group and $N_{i,j}^{EXP-HP}(r)$ is expected number of atom pairs at distance r for HP group as defined in Eq. 14.

Similarly energy score for HH group can be written as:

$$ES_{i,j,r}^{HH} = -\ln(N_{obs-HH}(i,j,r) / N_{i,j}^{EXP-HH}(r)) \quad (18)$$

where $ES_{i,j,r}^{HH}$ is the energy score of atom pair i^{th} and j^{th} at distant bin r for group HH, $N_{obs-HH}(i,j,r)$ is the observed number of atom pair i^{th} and j^{th} at distant bin r for HH group and $N_{i,j}^{EXP-HH}(r)$ is expected number of atom pairs at distance r for HH group as defined in Eq. 15.

Finally energy score for PP group can be written as:

$$ES_{i,j,r}^{PP} = -\ln(N_{obs-PP}(i,j,r) / N_{i,j}^{EXP-PP}(r)) \quad (19)$$

where $ES_{i,j,r}^{PP}$ is the energy score of atom pair i^{th} and j^{th} at distant bin r for group PP, $N_{obs-PP}(i,j,r)$ is the observed number of atom pair i^{th} and j^{th} at distant bin r for PP group and $N_{i,j}^{EXP-PP}(r)$ is expected number of atom pairs at distance r for PP group as defined in Eq. 16.

Later minimum energy or total energy of decoy set as well as native proteins are calculated from these energy score libraries. We use weight factors β_{hp}, β_{hh}, and β_{pp} to optimize the contribution of each of the three energy score libraries. So, total energy (TE) of the protein conformation can be written as:

$$TE = \beta_{hp} E_{hp} + \beta_{hh} E_{hh} + \beta_{pp} E_{pp} \quad (20)$$

where β_{hp}, β_{hh}, and β_{pp} are 3D weights of contribution and E_{hp}, E_{hh}, and E_{pp} are the energy scores obtained from three groups HP, HH and PP. Here E_{hp} can be written as:

$$E_{hp} = \sum_{i,j,r} ES_{i,j,r}^{HP} \tag{21}$$

Similarly, E_{hh} can be written as:

$$E_{hh} = \sum_{i,j,r} ES_{i,j,r}^{HH} \tag{22}$$

And, E_{pp} can be written as:

$$E_{pp} = \sum_{i,j,r} ES_{i,j,r}^{PP} \tag{23}$$

We use Genetic Algorithm (GA) for determining the best possible values of alpha (α_{hp}, α_{hh} and α_{pp}), and optimized the contributions of each of the three group by determining their appropriate weights β_{hp}, β_{hh}, and β_{pp} along with the z-score to discriminate the native from their decoys, where z-score of native structure is defined as:

$$Z = \frac{E_{native} - E_{average}}{E_{SD}} \tag{24}$$

where E_{native} is the energy of native protein, $E_{average}$ is the average energy of decoy sets corresponding to the same protein excluding native protein itself and E_{SD} is the standard deviation of the energies of all the decoy sets corresponding to the same protein.

In the optimization using GA, the value of alpha and beta ranges from 0 to 2 and -2 to 2 respectively. GA parameters were set as *i)* population size of 50, *ii)* single-point crossover and mutation, *iii)* elite rate of 5%, *iv)* crossover rate of 90% and v) mutation rate of 50%. Scores were optimized based on 3 decoy sets: Moulder, Rosetta and Tasser.

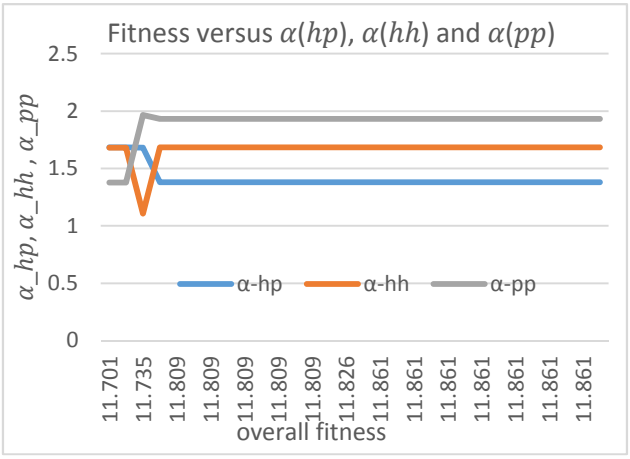

Figure 2: Fitness versus α_hp, α_hh and α_pp values. The values remain stable during optimization, ensure reliabilities.

The obtained best values of alphas are: α_{hp} = 1.3802541, α_{hh} = 1.6832844 and α_{pp} = 1.9315737. The obtained best beta values are β_{hp} = 1.4921875, β_{hh} = 0.55859375 and β_{pp} = 0.265625. Plot of obtained fitness versus α_{hp}, α_{hh} and α_{pp} values at each generation in Fig.2 shows the GA performance on selecting best fitness and also consistency of obtained fitness with values of α_{hp}, α_{hh} and α_{pp}.

GA over Grid Search for Optimal Parameter

In context of this application, search for optimal parameter involves *i)* generating 3D energy score libraries each time for 3D alpha values and *ii)* computing correct count and z-score of three decoy sets Moulder, Rosetta and Tasser each time for 3D beta values. Our goal is to obtain the best value of 3D alpha and 3D beta which provides us the maximum correct count for each of the decoy sets and high negative z-score. Generating 3D energy score libraries involve processing of 4332 native protein structures residing in hard drive. In addition, computing correct count and z-score of three decoy sets Moulder, Rosetta and Tasser involves processing of 20, 58 and 56 proteins respectively. Each of these proteins have around 600 decoy files on an

average and so, on an average we need to process 80,400 files. Thus, on each iteration we need to process 84,732 structure files.

Furthermore, our application involves obtaining optimal parameter for 3D alpha values as well as 3D beta values, totaling to 6 variables needed to be optimized. We choose GA to tackle this search problem involving multiple variables and huge I/O (Input/Output) operation over Grid Search because, GA searches for the global optima and converses quickly or in other words provides the results in few steps as shown in Fig. 2 whereas, Grid Search involves nested loop search. As our search space involves 3D alpha and 3D beta variables ranging from 0 to 2 and -2 to 2 respectively the Grid Search based approach involves 6 nested loops and each iteration involves huge I/O operations. In addition, Grid Search involves step size which is of greater importance, if we select a step size of greater width there exist a possibility of missing the optimal value whereas, if we use a finer grid search (small step size such as 0.01) we might end up running the process for months. Thus to obtain better result in considerable amount of time we selected GA over Grid Search based approach for optimal parameter search.

To access the performance of our 3DIGARS energy function we tested it with most challenging decoy sets as well as moderately challenging decoy sets in Table 3 against the state of art approaches DFIRE, RWplus, dDFIRE and DFIRE2.0 based on the number of correctly identified proteins and average z-score for three different decoy sets.

DATASET COLLECTION and DECOY DATASETS

Training Dataset

Datasets to generate energy score were obtained from three different sources, PDB (Protein Data Bank) server, ccPDB [28] (Compilation and Creation of datasets from PDB) server and PISCES [29] (A protein sequence culling server) server. Primarily we collected proteins with multiple chains

obtained from all experimental method, structures better than 1.5 Å resolution, R-factor of 0.0 to 0.25, chain length 40 or more and less than or equal to 30% sequence identity cutoff from all the three sources mentioned above.

Performance of these long multiple chain sequence datasets were very poor which lead us to exhaustively generate many different datasets with different specifications. Poor results from multiple and long chain dataset lead us towards some research for less number of chains and shorter chain length sequences. We generated dataset with number of chain 0 to 2 with maximum chain length of 1000, results from this specification was similar to the result obtained from multiple and long chain sequences. Later we collected dataset with minimum resolution 0.0 and maximum resolution 1.5, similarity cutoff 30%, single chain and maximum chain length of 500. This single chain and shorter length protein sequences gave us comparably better result than multiple chain. Thus we focused our research on single chain proteins. As we moved from multiple chain sequences to single chain we continued working only with PDB dataset because, we were unable to collect only single chain sequences from PISCES and ccPDB servers.

We exhaustively generated many single chain datasets with different specifications. To generate dataset less than or equal to 25% sequence identity we used a sequence clustering program BLASTCLUST [30]. While executing BLASTCLUST we found that it fails if the sequence length is less than 7 reside long and if the sequences have "X" or "U" (unknown residue) in a sequence. Additionally, it fails if there are more than 4 protein id's with different chain id's (>10jh_A, >10jh_B, >10jh_C, >10jh_D, >10jh_E and so on) in a FASTA input file. It also fails if four or more sequences are exactly same. To overcome BLASTCLUST problems we have an in-house program to remove the sequences that are shorter (< 7 residues) and also sequence containing unknown residues from the FASTA input file.

Furthermore, we also wrote a program which removes proteins with missing residues in the middle of the protein sequence. However, the program does not ignore the sequence if it has missing residues at terminals (5 residues from each end). Thus our final training dataset consist of only single chain protein sequences which are purified not to contain any proteins consisting of missing residues anywhere except the terminal regions. We generated purified dataset keeping all other specification common besides maximum resolution ranging from 1.5 to 2.5 and sequence identities cutoff, of 25%, 30%, 40%, 50%, 70% and 100%. The best result overall of these combination is obtained from collection of 4332 proteins from PDB which are single chain, missing residue purified, has 100% sequence identity cutoff, minimum resolution of 0.0 and maximum resolution of 2.5 and R-free of 0.25. This best collection before purification for missing residues had 10602 proteins. The results obtained from 70% sequence identity cutoff is very close to the result obtained from 100% sequence identity with later having slight improvement. Selecting proteins with 100% identity cutoff mean we are actually preserving actual representation of frequency distribution of amino acids in nature. This result suggest us that the current PDB has huge collection of proteins now, which is sufficient to gives us proper frequency distribution of the atom pairs in nature. Results obtained from all of the above specifications are mentioned in Table 2.

Decoy Datasets

Performance of 3DIGARS was evaluated on 11 different decoy datasets which are described in brief below. Three decoy sets Moulder, Rosetta and Tasser among the set of 11 decoys are considered to be the most challenging decoys.

Moulder Decoy-set

Moulder [31] decoy set consist of 20 proteins for which 300 comparative models were built using homologous template. The models were build using alignment that did not shared more than 95% of identically aligned positions or had at least 5 different alignment positions. These decoys were build using MODELLER-6 program which applied default model building routine with fastest refinement which keeps most of the template structure unchanged and are different from decoys that are generated by ab initio folding that have all structure regions reassembled from scratch.

Rosetta Decoy-set

Decoy set for 58 proteins were generated by Baker Lab which contains 20 random models and 100 lowest scoring models from 10,000 decoys using ROSETTA de novo structure prediction followed by all-atom refinement [32]. Current Rosetta decoy set has been improved than the original Rosetta decoy set by adding side chains to the centroid/backbone models and refining the structures to remove steric clashes. The improvement over original Rosetta were based on four important points required to generate optimal decoy sets 1) decoy set should contain conformations for a wide variety of different proteins to avoid over fitting; 2) decoy set should contain conformation close to (< 4Å) to the native structure; 3) decoy set should consist of conformations that are at least near local minima of energy potential; and 4) decoy set should be produced without using information from native structure [33].

I-Tasser Decoy-set-II

I-Tasser [34] decoy set-II were generated first by using Monte Carlo Simulations and then refined by GROMACS4.0 MD simulation to remove steric clashes and improve hydrogen-bonding

network [34]. This set contains of 56 proteins each of which contains 300-500 decoys generated by both template-based modeling and atomic-level structure refinement.

4state_reduced

This decoy set consist of 7 proteins. The CA positions for these decoys were generated by choosing ten residues in each protein using a 4-state off-lattice model. All atom models were built from the CA atoms with the program segmod [35].

Fisa

This set contains decoys for four small alpha-helical proteins. Main chains were generated using a fragment insertion simulated annealing procedure [Simons et al] whereas side chains were modelled with SCWRL package [36].

Fisa_casp3

This set contains 5 proteins. It contains decoys for proteins predicted by the Baker group for CASP3. Main chain for these decoys were also generated using a fragment insertion simulated annealing procedure whereas side chains were modelled with SCWRL package [36].

Hg_structal

This set contains decoys for 29 globins. Each proteins is built by comparative modelling using 29 other globins using [37].

Ig_structal

This set contains 61 immunoglobulins each of these is built by comparative modelling suing all the other immunoglobulins as templates using segmod program [37].

Ig_structal_hires

This set contains 20 immunoglobulins which is high resolution subset of immunoglobulins decoy set. The resolution range for this set is 1.7-2.2 Å compared to full 61 set which has resolution range from 1.7-3.1 Å. These sets are also build by comparative modeling using all other immunoglobulins as templates using segmod program [37].

Lattice_ssfit

This set contains eight small proteins generated by ab initio methods [38].

Lmds

The local minima decoy set (lmds) contains of ten proteins derived from experimental secondary structures of ten small proteins that belong to diverse structural classes. Two of the proteins were CASP3 targets [39].

Decoy sets 4state_reduced, fisa, fisa_casp3, hg_structal, ig_structal, ig_structal_hires, lattice_ssfit and lmds were obtained from http://dd.compbio.washington.edu/.

RESULTS

During our search for the best training dataset, we calculated the correct count of most challenging decoy set by applying two different reference state to the collection of the dataset. Table 2 implicates the exhaustive search of best dataset. The best correct count combination for MOULDER, ROSETA, and TASSER was obtained from the training dataset with resolution 1.5 and sequence similarity 100% which is **19, 23, 46** respectively (see Table 2). This motivated us to select the dataset with sequence similarity 100% and maximum resolution ranging from 1.5 to 2.5 as a training dataset for hydrophobic and hydrophilic based energy function (3DIGARS).

From Table 2 we can also see that DFIRE based energy function outperforms RAPDF based energy function which motivated us towards improvement over DFIRE based reference state.

Table 2: Performance of two different reference state on training dataset differed by maximum resolution and similarity cutoff while keeping other parameters such as experimental method as "Ignore", molecule type as "Protein", refinement R-free of minimum 0.0 and maximum 0.25 , number of chains as "Single Chain" if not mentioned.

S.No.	Training Set	RAPDF Results			DFIRE Results		
		M	**Ro**	**T**	**M**	**Ro**	**T**
1	R = 3.0, C = 30%	19	9	41	19	20	46
2	R = 2.5, C = 40%	19	5	42	19	18	43
3	R = 2.0, C = 50%	19	6	41	19	15	42
4	R = 2.5, C = 50%	19	6	41	19	16	43
5	R = 2.5, C = 70%	19	9	41	19	20	44
6	R = 2.5, C = 100%	19	8	40	19	19	46
7	R = 1.5, C = 100%	19	9	41	**19**	**23**	**46**
8	R = 3.0, C = 100%	19	7	41	19	19	45
9	R = 1.5, C = 30%, CL = 500	19	8	42	19	21	46
10	R = 1.5, C = 25%, MC	19	6	42	19	13	38
11	R = 1.5, C = 30%, MC	19	7	43	19	16	42
12	R = 1.5, C = 40%, MC	19	6	42	19	13	36
13	SC, R = 2.5, C = 100% and MC, R = 1.5, C = 25% combined	19	8	42	19	17	43

M- moulder
Ro- rosetta
T- tasser
R- maximum resolution
C- similarity cutoff
CL- chain length
MC- multiple chain
SC- single chain
Moulder Total Targets: 20, Rosetta Total Targets: 58, Tasser Total Targets: 56. DFIRE results are based on the DFIRE reference state with alpha = 1.57.

Furthermore, in Table 3 value within the parenthesis are average z-scores of the native structures and values outside of parenthesis are number of correct count. Here the term correct count can be described as the number of correctly identified native proteins from its decoy sets. Good energy function is the one which can assign highest energy to the native proteins compared to its decoy sets and thus is able to classify native proteins from its decoy sets more efficiently. In other words correct count implicates that an efficient energy function can identify more native proteins from the collection of native and its decoy sets. Results for DFIRE, RWplus and

dDFIRE are obtained from the GOAP: A Generalized Orientation-Dependent, All-Atom Statistical Potential from Protein Structure Prediction [40]. Correct count and z-score for DFIRE2.0 is computed from DFIRE2.0 package freely available from the Sparks Lab online server [41]. Correct counts by (3DIGARS) is calculated using energy score libraries generated using the dataset with resolution 1.5, sequence similarity cutoff of 100%, keeping all other parameters used for data collection common as described in DATASET section above. Table 3 clearly shows that hydrophobic and hydrophilic based energy function outperform DFIRE, RWplus, dDFIRE and DFIRE2.0 based energy functions for most challenging Rosetta decoy-set and also for decoy-set fisa_casp3. It is to be noted that RWplus computed 56 out of 56 for their own designed Tasser decoy-set, which could be a special case, as it is not consistently better in other cases.

Table 3: Comparison between DFIRE, RWplus, dDFIRE, DFIRE2.0 and our energy function (3DIGARS) on 11 decoy sets based on correct selection of native from their decoy set and z-score.

Decoy Sets	DFIRE	RWplus	dDFIRE	DFIRE2.0	3DIGARS	No. of targets
Moulder	19 (-2.97)	19 (-2.84)	18 (-2.74)	19 (-2.705631)	19 (**-2.99805**)	20
Rosetta	20 (-1.82)	20 (-1.47)	12 (-0.83)	22 (-1.759141)	**31** (**-2.02284**)	58
Tasser	49 (-4.02)	56 (-5.77)	48 (-5.03)	53 (-4.548973)	53 (-4.03677)	56
4state_reduced	6 (-3.48)	6 (-3.51)	7 (-4.15)	6 (-3.166685)	6 (-3.37116)	7
Fisa	3 (-4.87)	3 (-4.79)	3 (-3.80)	3 (-4.602856)	3 (-4.59109)	4
Fisa_casp3	4 (-4.80)	4 (-5.17)	4 (-4.83)	4 (-5.083463)	**5** (-4.3191)	5
Hg_structal	12 (-1.97)	12 (-1.74)	16 (-1.33)	12 (-1.823197)	12 (-1.91381)	29
Ig_structal	0 (0.92)	0 (1.11)	26 (-1.02)	0 (0.987806)	0 (0.644978)	61
Ig_structal_hires	0 (0.17)	0 (0.32)	16 (-2.05)	0 (0.226042)	0 (-0.00237)	20
Lattice_ssfit	8 (-9.44)	8 (-8.85)	8 (-10.12)	8 (-7.128327)	8 (-5.9903)	8
lmds	7 (-0.88)	7 (-1.03)	6 (-2.44)	7 (-0.715411)	7 (-1.96151)	10
Total	128 (-1.94)	135 (-2.13)	164 (-2.52)	134 (-2.75635)	144 (**-2.77837**)	278

Bold indicates the best among closest state-of-arts methods

Additionally, it is found that not all the state-of-art approaches perform better on Moulder, Rosetta and I-Tasser decoy sets. This implicates that - Moulder, Rosetta and I-Tasser decoy sets are the most challenging among the 11 different decoy sets listed above. This motivated us to optimize our energy function on these three most challenging decoy sets which

resulted in improved results. Our future goal is to incorporate the missing features (if any) and then to optimize our energy function on all the available decoy sets and we believe that further optimization will lead us to better results. Table 4 presents separately highlights the performance of 3DIGARS on three most challenging decoy sets Moulder, Rosetta and I-Tasser. 3DIGARS is found to be very competitive and based on the most challenging Rosetta decoy set, 3DIGARS outperforms the nearest competitor by 40.9%.

Table 4: Comparison between DFIRE, RWplus, dDFIRE, DFIRE2.0 and our energy function (3DIGARS) based on correct selection of native from their decoy set and z-score.

Decoy Sets	DFIRE	RWplus	dDFIRE	DFIRE2.0	3DIGARS	No. of targets
Moulder	**19** (-2.97)	**19** (-2.84)	18 (-2.74)	**19** (-2.71)	**19** (**-2.998**)	20
Rosetta	20 (-1.82)	20 (-1.47)	12 (-0.83)	22 (-1.76)	**31** (**-2.023**)	58
Tasser	49 (-4.02)	**56** (**-5.77**)	48 (-5.03)	53 (-4.548)	53 (-4.036)	56

Bold indicates best score and underline indicates competitive score.

CONCLUSIONS

Identifying native proteins from their decoy sets have always been a challenging task. While exercising with the two different reference state implementation, RAPDF and DFIRE, we formulated a better energy function based on the training dataset, hydrophobic and hydrophilic property of amino acid and their role in 3D structure formation, 3D values of alpha based on hydro-phobic and hydrophilic residues spatial distributions and optimized weights for each of the three combinations along with the z-score for discriminating the native from the decoys.

The most important contribution we made is the extension of the concept of ideal gas reference state by constructing three energy score libraries based on hydrophobic and hydrophilic residue's spatial distribution within protein conformations. Each of the three category of residues is given their independent and more appropriate semi-spherical distribution parameter

alphas, and then we determine their best values instead of having a single parameter based gross average inaction model.

During our research we also found that training dataset with different specification produce nearly similar results. Nevertheless, the performance of the training dataset with sequence similarity cutoff 100% and resolution ≤ 2.5 outperforms all other training dataset with different specifications. This indicates that keeping 100% similar dataset helps us maintain the natural frequency distributions and help develop better energy function.

We compare the performance of our proposed 3DIGARS with the state-of-art-approaches DFIRE, RWplus, dDFIRE and DFIRE2.0 using the most challenging three different decoy datasets as well as eight moderately challenging decoy datasets. 3DIGARS is found to be very competitive and based on the most challenging dataset Rosetta, 3DIGARS outperforms the nearest competitor by 40.9% and is also consistent with other decoy sets.

SUPPLEMENTARY CONTENT

The software, dataset and related material is available free of charge via the Internet at http://cs.uno.edu/~tamjid/Software/3DIGARS/3DIGARS.zip

REFERENCES

1. Lu, H. & Skolnick, J. (2001). A Distance-Dependent Atomic Knowledge-Based Potential for Improved Protein Structure Selection. *Proteins: Struct., Funct., Genet.* **44**, 223-232.
2. Moult, J. (1997). Comparison of Database Potentials and Molecular Mechanics Force Fields. *Curr Opin in Str Bio.* **7**, 194-199.
3. Vajda, S., Sippl, M. & Novotny, J. (1997). Empirical Potentials and Functions for Protein Folding and Binding. *Curr Opin in Str Bio.* **7**, 222-228.
4. Hao, M.-H. & Scheragat, H. A. (1999). Designing Potential Energy Functions for Protein Folding. *Curr Opin in Str Bio.* **9**, 184-188.
5. Miyazawa, S. & Jernigan, R. L. (1999). An Empirical Energy Potential with a Reference State for Protein Fold and Sequence Recognition. *Proteins: Struct., Funct., Genet.* **36**, 357-369.
6. Lazaridis, T. & Karplus, M. (2000). Effective Energy Functions for Protein Structure Prediction. *Curr Opin in Str Bio.* **10**, 139-145.

7. Cornell, W. D., Cieplak, P., Bayly, C. I., Gould, I. R., Merz, K. M., Ferguson, D. M., Spellmeyer, D. C., Fox, T., Caldwell, J. W. & Kollman, P. A. (1995). A Second Generation Force Field for the Simulation of Proteins, Nucleic Acids, and Organic Molecules. *J. Am. Chem. Soc.* **117**, 5179-5197.
8. Brooks, B. R., Bruccoleri, R. E., Olafson, B. D., States, D. J., Swaminathan, S. & Karplus, M. (1983). CHARMM: A Program for Macromolecular Energy, Minimization, and Dynamics Calculations. *J. Comput. Chem.* **4**, 187-217.
9. Samudrala, R. & Moult, J. (1997). An All-atom Distance-dependent Conditional Probability Discriminatory Function for Protein Structure Prediction. *J. Mol. Biol.*, 895-916.
10. Zhou, H. & Zhou, Y. (2002). Distance-scaled, Finite Ideal-gas Reference State Improves Structure-derived Potentials of Mean Force for Structure Selection and Stability Prediction. *Protein Sci.*, 2714–2726.
11. Tanaka, S. & Scheraga, H. A. (1976). Medium- and Long-Range Interaction Parameters between Amino Acids for Predicting Three-Dimensional Structures of Proteins. *Macromolecules* **9**, 945-950.
12. Jernigan, R. L. & Bahar, I. (1996). Structure-Derived Potentials and Protein Simulations. *Curr Opin in Str Bio.* **6**, 195-209.
13. Koretke, K. K., Luthey-Schulten, Z. & Wolynes, P. G. (1996). Self-Consistently Optimized Statistical Mechanical Energy Functions for Sequence Structure Alignment. *Protein Sci.* **5**, 1043-1059.
14. Tobi, D. & Elber, R. (2000). Distance-Dependent, Pair Potential for Protein Folding: Results From Linear Optimization. *Proteins: Struct., Funct., Bioinf.* **41**, 40-46.
15. Deng, H., Jia, Y., Wei, Y. & Zhang, Y. (2012). What is the Best Reference State for Designing Statistical Atomic Potentials in Protein Structure Prediction? *Proteins: Struct., Funct., Bioinf.* **80**, 2311–2322.
16. Kortemmea, T., Morozova, A. V. & Baker, D. (2003). An orientation-dependent hydrogen bonding potential improves prediction of specificity and structure for proteins and protein-protein complexes. *Journal of Molecular Biology* **326**, 1239-1259.
17. Zhou, H. & Zhou, Y. (2002). Distance-scaled, finite ideal-gas reference state improves structure-derived potentials of mean force for structure selection and stability prediction. *Protein Science* **11**, 2714-2726.
18. Yang, Y. & Zhou, Y. (2008). Specific interactions for ab initio folding of protein terminal regions with secondary structures. *PROTEINS: Structure, Function, and Bioinformatics* **72**, 793-803.
19. Lu, M., Dousis, A. D. & Ma, J. (2008). OPUS-PSP: an orientation-dependent statistical all-atom potential derived from side-chain packing. *Journal of Molecular Biology* **376**, 288-301.
20. Zhang, J. & Zhang, Y. (2010). A Novel Side-Chain Orientation Dependent Potential Derived from Random-Walk Reference State for Protein Fold Selection and Structure Prediction. *PLoS ONE* **5**, e15386.
21. Zhou, H. & Skolnick, J. (2011). GOAP: A Generalized Orientation-Dependent, All-Atom Statistical Potential for Protein Structure Prediction. *Biophysical Journal* **101**, 2043–2052.
22. Hoque, M. T., Chetty, M. & Sattar, A. (2007). Protein Folding Prediction in 3D FCC HP Lattice Model Using Genetic Algorithm In *Bioinformatics special session, IEEE Congress on Evolutionary Computation (CEC)*, Singapore.
23. Fidanova, S. (2010). An Improvement of the Grid-based Hydrophobic-Hydrophilic Model. *Int. J. Bioautomation* **14**, 147-156.
24. Hoque, T., Chetty, M. & Sattar, A. (2009). Extended HP Model for Protein Structure Prediction. *J. Comput Biol* **16**, 85-103.

25. Hoque, T., Chetty, M. & Sattar, A. (2007). Protein folding prediction in 3D FCC HP lattice model using genetic algorithm. *IEEE Congress on Evolutionary Computation (CEC) Singapore*, 4138-4145.
26. Hoque, M. T., Chetty, M., Lewis, A., Sattar, A. & Avery, V. M. (2010). DFS Generated Pathways in GA Crossover for Protein Structure Prediction. *Neurocomputing, Elsevier*
27. PDB, R. Advanced Search Interface., Vol. 2014, pp. Web. February 2014. http://www.rcsb.org/pdb/search/advSearch.do.
28. Singh, H., Chauhan, J. S., Gromiha, M. M., Consortium, O. S. D. D. & Raghava, G. P. S. (2011). ccPDB: Compilation and Creation of Data Sets from Protein Data Bank. *Nucleic Acids Research* **40**.
29. Lab, D. (1969). Taking Input Parameters for Culling Whole PDB, Vol. 2014, pp. Web. February 2014. http://dunbrack.fccc.edu/Guoli/PISCES_ChooseInputPage.php.
30. Altschul, S. F., Gish, W., Miller, W., Myers, E. W. & Lipman, D. J. (1990). Basic Local Alignment Search Tool. *J. Mol. Biol.* **215**, 403-410.
31. Sali, A. Decoy Models., Vol. 2014, pp. Web. July 2014. http://salilab.org/john_decoys.html.
32. Zhang, J. & Zhang, Y. (2010). A Novel Side-Chain Orientation Dependent Potential Derived from Random-Walk Reference State for Protein Fold Selection and Structure Prediction. *Plos One* **5**.
33. Tsai, J., Bonneau, R., Morozov, A. V., Kuhlman, B., Rohl, C. A. & Baker, D. (2003). An Improved Protein Decoy Set for Testing Energy Functions for Protein Structure Prediction. *Proteins: Struct., Funct., Bioinf.* **53**, 76-87.
34. Lab, Z. Protein Structure Decoys., Vol. 2014, pp. Web. July 2014. http://zhanglab.ccmb.med.umich.edu/decoys/. Zhang Lab.
35. Park, B. & Levitt, M. (1996). Energy Functions that Discriminate X-ray and Near-native Folds from Well-constructed Decoys. *J. Mol. Biol.* **258**, 367-392.
36. Simons, K. T., Kooperberg, C., Huang, E. & Baker, D. (1997). Assembly of Protein Tertiary Structures from Fragments with Similar Local Sequences using Simulated Annealing and Bayesian Scoring Functions. *J. Mol. Biol.* **268**, 209-225.
37. Levitt, M. Accurate Modeling of Protein Conformation by Automatic Segment Matching, Vol. 2014, pp. Web. July 2014. http://www.ncbi.nlm.nih.gov/pubmed/1640463.
38. Samudrala, R., Xia, Y. & Levitt, M. (1999). A Combined Approach for Ab Initio Construction of Low Resolution Protein Tertiary Structures From Sequences. *Pac Symp Biocomput*.
39. Keasar, C. & Levitt, M. (2003). A Novel Approach to Decoy Set Generation: Designing a Physical Energy Function Having Local Minima with Native Structure Characteristics. *J. Mol. Biol.* **329**, 159-174.
40. Zhou, H. & Skolnick, J. (2011). GOAP: A Generalized Orientation-Dependent, All-Atom Statistical Potential for Protein Structure Prediction. *Biophys. J .* **101**, 2043-2052.
41. Yang, Y. Download Page., Vol. 2014, pp. Web. June 2014. http://sparks-lab.org/yueyang/download/index.php.

VITA

The author Avdesh Mishra was born in Udayapur, Banke District Nepal. He obtained his Bachelor's degree in computer engineering from Tribhuvan University in 2012. He joined the University of New Orleans computer science graduate program to pursue a MS degree with concentration in Bioinformatics. This research work was done under the supervision of Dr. Tamjidul Hoque in 2015.